Research article

Understand Noise on Universal Quantum Adder Circuit

Wiphoo Methachawalit* and Prabhas Chongstitvatana

Department of Computer Engineering, Faculty of Engineer, Chulalongkorn University, Bangkok, Thailand

Curr. Appl. Sci. Technol. xxxx, Vol. xx (No. x), e0255872; https://doi.org/10.55003/cast.2023.255872

Received: 3 October 2022, Revised: 23 March 2023, Accepted: 28 September 2023 Published:14 December 2023

Keywords

quantum computing;

adder circuit;

quantum noise

Abstract

Quantum Fourier Transform (QFT) is an essential algorithm for quantum computers. There are many uses of QFT in the application of quantum computing. In this work, we proposed a generalized adder circuit that was fundamental for QFT. We designed and ran the experiments with the proposed adder circuit on an IBM quantum computer facility. We observed that the number of qubits was one factor in the error rate. We found that our proposed two-qubits adder circuit running on the IBM quantum computer had an error rate of around 25%. The complexity of the adder circuit includes qubit connectivity, physical devices, and error from noise due to the environment. We demonstrated the constraints of the proposed adder circuit.

1. Introduction

Quantum computing has experienced a surge in popularity and has garnered significant attention from both researchers and governmental bodies. It has proven to be a promising field with numerous powerful algorithms [1]. Notably, Shor's factorization algorithm [2] has gained widespread recognition and has the potential to revolutionize the encryption landscape [3]. Many efforts have been devoted to implementing Shor's algorithm on various quantum devices. For instance, Drapper [4] proposed an addition operation for quantum computers, while Vandersypen *et al*. [5] conducted experiments on prime factorization using a nuclear magnetic resonance quantum computer. Beauregard [6] put forward a circuit design for Shor's algorithm employing 2n+3 qubits. In recent years, IBM has made notable advancements in quantum computing by developing programmable superconducting-based quantum computers, offering the Open Quantum Assembly Language [7], and providing a quantum computer system for researchers. Progress has been made in terms of qubit count, qubit quality, and the overall size of quantum volumes, with ongoing improvements observed over time. Quantum volume, as a metric introduced by Cross *et al*. [8], serves to quantify the performance of a quantum computer within the noisy intermediate-scale quantum computing

*Corresponding author: Tel.: (+66) 0-2218-6956 Fax: (+66) 0-2218-6955
E-mail: 6170270321@student.chula.ac.th

(NISQ) paradigm. Our focus lies in the design of an adder circuit that serves as an integral component of the prime factorization circuit. We proposed a generalized adder circuit [9], which formed the foundation for quantum Fourier transform (QFT) [10, 11]. Additionally, we considered realistic parameters, such as noise, and incorporated them into our work to align with real-world quantum computing systems.

2. Materials and Methods

2.1 Quantum simulator and quantum computer

For our experiment, we utilized the open quantum platform provided by IBM [12] to access both the quantum simulator and the physical quantum computer. The Python Qiskit library [13] served as the interface to interact with the IBM quantum system. This library offers a software development kit that enabled us to simulate the behavior of the quantum computer on our local machine. Subsequently, we executed the developed circuit on the actual quantum computer. To ensure the realism of our experimental outcomes, we incorporated the noise and topology characteristics obtained from the IBM quantum computer into the simulator [14]. By doing so, we accounted for the impact of noise on the results, as it is an inherent factor affecting the performance of real quantum computers.

2.2 Quantum two-qubits adder circuit

In our study, we put forth a modified adder circuit that employs 2n+1 qubits for an n-qubit adder [9]. To validate its effectiveness, we conducted experiments using both IBM quantum simulators and real quantum computers. The IBM quantum computer provided us with valuable information concerning device calibration, including qubit gate and measurement errors. In the absence of noise within the simulator, the experimental results were consistently flawless across all cases. However, when implementing the adder circuit on the IBM quantum computers, the results exhibited errors in most cases. Despite these errors, the outcomes demonstrated the potential for correct addition, highlighting the promising capabilities of the approach. In this experiment, we used the circuit as shown in Figure 1.

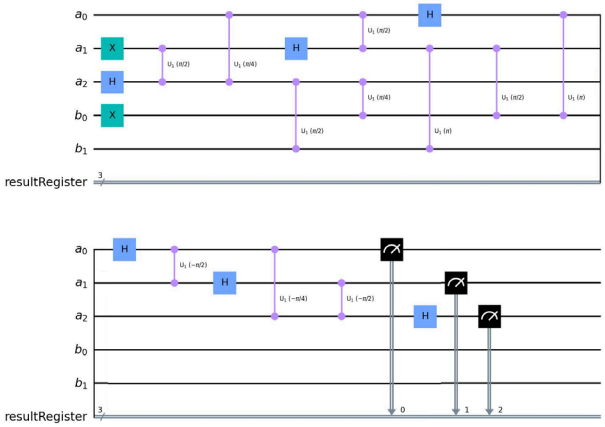

Figure 1. The two-qubits adder circuit for 10+01

2.3 IBM quantum computers

The IBM quantum computer is composed of interconnected physical qubits based on superconducting technology. These qubits are organized and connected in a graph-like structure known as the qubit topology or qubit connectivity. To manipulate these qubits and perform operations such as single-qubit rotations and two-qubit gates, IBM employs techniques including microwave pulses and electromagnetic fields. IBM is continuously developing new generations of quantum processors with varying numbers of qubits and evolving topologies. The number of qubits is increasing, and the topology has shifted from a nearly square lattice to a more refined configuration, resulting in reduced qubit connectivity [15].

The three primary properties of IBM quantum processors are the qubit coherence time, single-qubit and two-qubit manipulation errors, and readout errors. The qubit coherence time is a critical factor in constructing a quantum circuit and encompasses two metrics: relaxation time (T1) and dephasing time (T2). T1 measures the time it takes for a qubit to transition from its excited state |1> to the ground state |0>, while T2 measures the time it takes for a qubit in a superposition state |+> to lose its superposition. Figure 2 illustrates that the average T1 and T2 for the ibmq_quito processor are 97.99 microseconds and 89.84 microseconds, respectively. The coherence time of quantum processors is influenced by environmental noise, fabrication processes, material quality, and the microwave pulses used for qubit manipulation.

IBM employs various techniques, including microwave pulses, to manipulate physical single-qubits and two-qubit operations. However, they also provide a logical layer representation that allows researchers to manipulate qubits using gate operations without directly dealing with the physical aspects. This logical layer simplifies the process of understanding how to manipulate physical qubits through microwave pulses. An example of a single-qubit gate operation is the Pauli-X gate, also known as a bit-flip or NOT gate. A fundamental two-qubit gate operation is the CNOT (controlled not) gate [16]. Figure 2 presents the error rates for both single-qubit and two-qubit gate operations, as well as the average error rates for the ibmq_quito quantum processor due to imperfections in controlling the physical qubits. The average Pauli-X gate error is 3.518e-4, while the CNOT gate error is 1.118e-2. The error rate for two-qubit operations is notably higher than that for single-qubit operations. The error rates for two-qubits are also correlated with the complexity of the qubit topology. The heavy-hex lattice topology offers advantages in terms of fidelity and scalability as it reduces frequency collisions resulting from the qubits' resonance frequencies [15].

Readout refers to the process of measuring the state of a qubit. IBM utilizes attenuators, filters, and amplifiers to minimize noise during the readout of qubit signals [17]. Figure 2 indicates that the average readout error for the ibmq_quito processor has a possibility of 4.644e-2.

The available topologies for IBM's five-qubit quantum computers include linear and T-shaped configurations. The IBM quantum computing facility houses multiple computers with these topologies. For the linear topology, we selected the ibmq_manila [18] system, and for the T-shaped topology, we chose the ibmq_quito [19] system. The simulator experiments also utilize the topologies and error characteristics of the ibmq_manila and ibmq_quito systems.

2.4 Transpilation process

The transpilation process [20] refers to the conversion of logical gate operations into the physical manipulation of qubits within a specific physical quantum processor. In the case of our study, Qiskit performs transpilation on the proposed adder circuit for both the ibmq_quito and ibmq_manila quantum processors. The transpilation process comprises several steps, including virtual circuit optimization, decomposition of 3+ qubit gates, placement of gates on physical qubits, routing on

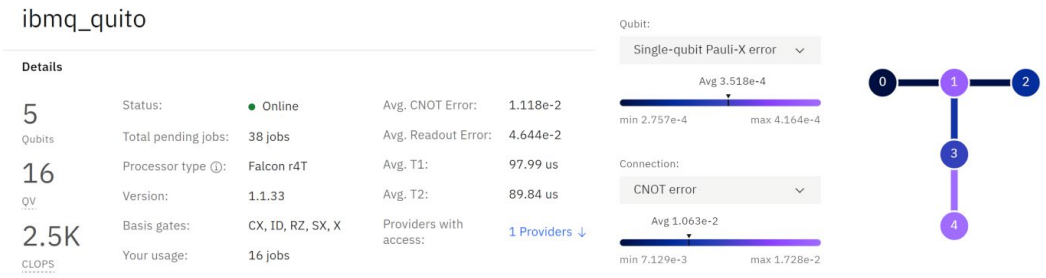

Figure 2. The ibmq_quito details include the number of qubits, available gates, and gate errors of a single-qubit and two-qubit [19].

restricted topologies, translation into basis gates, and physical circuit optimization. For this experiment, we did not perform any additional optimization beyond the default transpilation process.

To examine the effects of the transpiler, we compare three circuits before and after transpilation. Figure 3 illustrates how the transpiler converts the Hadamard gate into three basic gates (a rotation about the z-axis gate and a square root x gate) on the ibmq_quito computer. Figure 4 demonstrates how the transpiler converts the control rotation about the z-axis gate into five basic gates (a rotation about the z-axis gate and a controlled-NOT gate) on the ibmq_quito. Figure 5 represents the second part of our adder circuit, which involves the quantum Fourier transform. Figure 6 shows how the Qiskit library converts this circuit for the IBM ibmq_quito quantum computer. During this conversion process, three basic gates from ibmq_quito are added, including 18 CNOT gates, 14 Rotation Z gates, and 3 NOT gates.

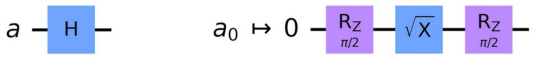

Figure 3. The representation of a Hadamard gate (left). The circuit after the transpilation process for ibmq_quito (right).

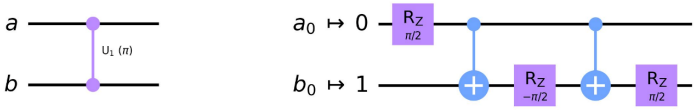

Figure 4. The representation of a CU1 (control rotation around the z-axis) gate (left). The circuit after the transpilation process for ibmq_quito (right).

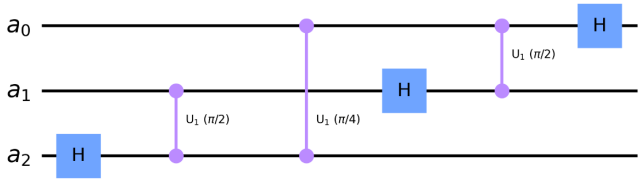

Figure 5. A part of the proposed adder circuit for quantum Fourier transform

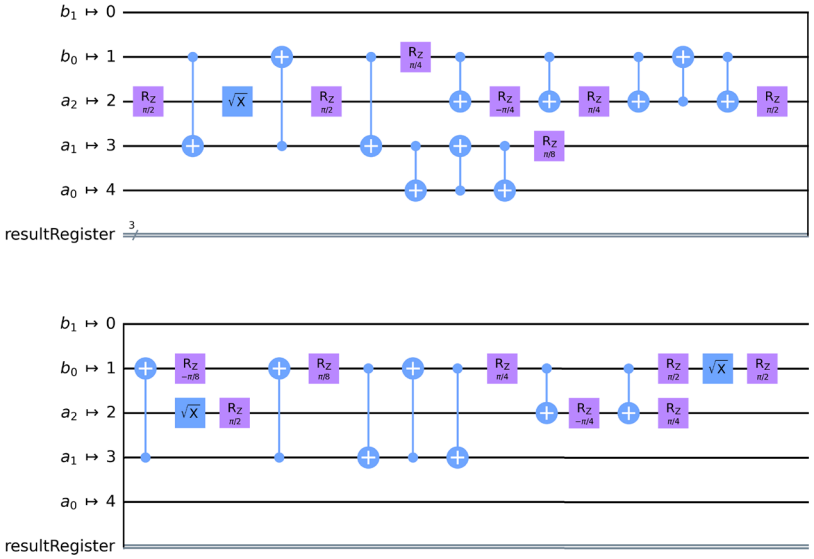

Figure 6. The transpiled circuit of Figure 5 for ibmq_quito computer

2.5 Experiment hypothesis and procedure

Understanding the physical layer of a quantum computer is crucial for constructing a generalized circuit [16]. The physical layer encompasses the control, measurement, and error correction of individual physical qubits. It involves knowledge about the properties of the quantum processor, such as coherence time, gate errors, readout errors, and topology. However, imperfections in fabrication, manipulation, connection, and environmental noise introduce significant uncertainties in the physical properties of a quantum computer.

In our experiments, we employed the adder circuit on a quantum simulator as well as two different IBM quantum computers with distinct qubit topologies, namely ibmq_quito and ibmq_manila. We used the generalized five-qubit adder circuit [9] to perform one and two bit additions with all possible input combinations. Before executing each experiment on an IBM quantum computer, we obtained the physical device calibration information, including the qubit topology, gate manipulation errors, and measurement errors. We took into account the physical device's properties such as topology, coherence time, gate operations, and readout errors from both processors. Our intention was to simulate an ideal scenario of the noise model based on the characteristics of ibmq_quito and ibmq_manila. By comparing the results obtained from the actual devices with the simulated noise model, we aimed to observe consistent outcomes that exhibited a small amount of noise similar to that of a real quantum device.

3. Results and Discussion

3.1 Results

The experimental results were obtained using an IBM quantum simulator with multiple noise models and actual IBM quantum computers. The noise models used in the simulation were based on measurements taken during the experiments conducted on the IBM quantum computers. The

magnitude of errors observed in the results depended on the specific noise characteristics of each quantum computer. Figures 7 to 10 present the outcomes of the experiments

Figure 7 and Figure 9 depict the results of the simulation experiments incorporating the noise models from ibmq_quito and ibmq_manila, respectively. In these Figures, the X-axis represents the two input numbers in binary, while the Y-axis represents the probability of the adder producing the correct result. A probability of 1 signifies that the adder always correctly performs the addition. The experiments were repeated 2,048 times for each input combination.

The results of the one-qubit addition with the noise models from ibmq_quito and ibmq_manila are relatively similar. The average peak probabilities of correctly adding the two inputs are around 0.855 for ibmq_quito and 0.8825 for ibmq_manila (Figure 8). Although there are some minor errors, the noise models do not significantly impact the expected results.

In contrast, the two-qubit addition yields different outcomes. The average probability of correctly adding the two inputs is lower, with around 0.39875 for ibmq_quito and 0.255 for ibmq_manila (Figure 10). However, at the peak probability, the result is correct. It is important to note that the two-qubit addition exhibits a higher error rate compared to the one-qubit addition

Considering the actual experiments performed on the quantum computers, the results align with the simulations. For the one-qubit addition, both ibmq_quito and ibmq_manila demonstrate correct results for all inputs, with peak probabilities ranging from 0.84 to 0.91 (Figure 8). However, for the two-qubit addition, ibmq_quito performs relatively better than ibmq_manila. Although there are 12 cases (01+10, 10+11, 11+10, and 11+11) where the peak probabilities are lower than 0.5, ibmq_quito still shows a higher probability of correct results compared to ibmq_manila (Figure 10).

In summary, both ibmq_quito and ibmq_manila, when utilized with the proposed generalized adder circuit for one-qubit addition, produce correct results for all input combinations. The two-qubit adder circuit on ibmq_quito exhibits peak probabilities at the correct output results for all inputs, albeit with a decrease in probability compared to the one-qubit addition. On the other hand, ibmq_manila demonstrates 12 peak probabilities at the correct results, with an overall correctness rate of approximately 75%.

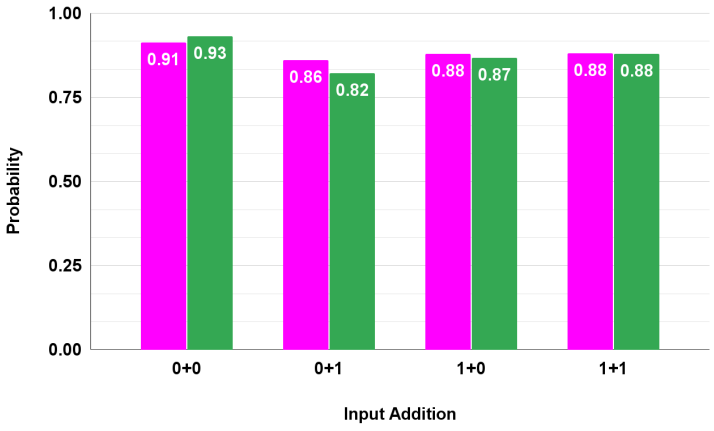

Figure 7. The probability of the correct result from the simulation on a one-qubit addition (with noise). The ibmq_quito result is light magenta, and the ibmq_manila result is dark green.

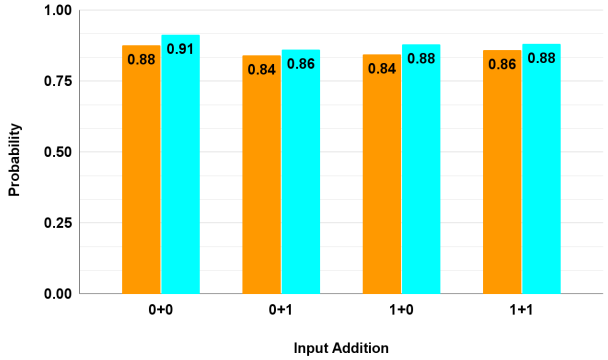

Figure 8. The probability of the correct result from the actual IBM quantum on a one-qubit addition. The ibmq_quito is dark orange, and the ibmq_manila is light cyan.

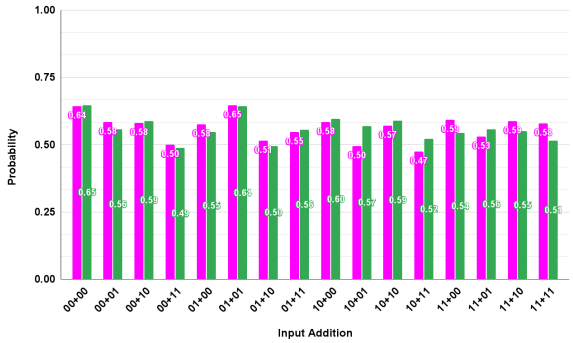

Figure 9. The probability of the correct result from the simulation on a two-qubits addition (with noise). The ibmq_quito result is light magenta, and the ibmq_manila result is dark green.

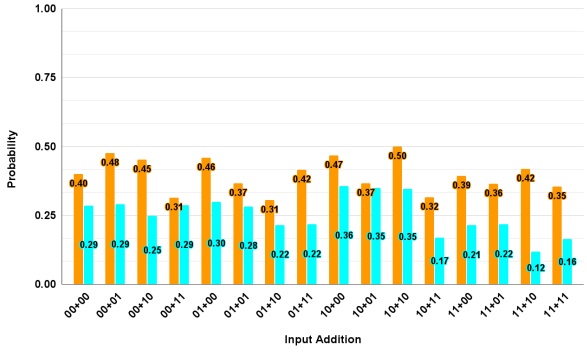

Figure 10. The probability of the correct result from the actual IBM quantum on a two-qubits addition. The ibmq_quito is dark orange, and the ibmq_manila is light cyan.

3.2 Discussion

The results of the experiments validate the correctness of the proposed generalized two-qubit adder circuit when executed on IBM quantum computers. Compared to previous experiments conducted on deprecated quantum computers like ibmq_essex, ibmq_yorktown, and ibmq_melbourne, the adder circuit performs better on the current IBM quantum computers, namely ibmq_quito and ibmq_manila. However, direct comparison with the deprecated quantum computers is not possible due to the lack of calibration information (gate and measurement errors) for those devices.

The improvement observed in the IBM quantum computers can be attributed to two factors. Firstly, it could be a result of advancements in the physical devices themselves. The deprecated quantum computers may have had limitations or imperfections that have since been addressed in the newer models. Unfortunately, without specific calibration data, a direct comparison is not feasible.

The second factor contributing to the improvement is the Qiskit transpilation process, which converts the adder circuit to be executed on the physical devices. This process involves various optimization steps, such as gate decomposition, qubit placement, routing, and gate translation. However, it should be noted that adding gates during the transpilation process can introduce additional errors to the adder circuit.

Understanding the transformation from a logical quantum circuit to the manipulation of physical qubits is crucial for researchers to investigate and improve the accuracy of their results on real devices. While certain limitations such as fabrication imperfections and the use of microwave pulses for qubit manipulation cannot be directly addressed, the concept of error-correcting codes holds the potential for improving the accuracy of computations on noisy or large-scale quantum computers. However, implementing error-correcting codes requires additional ancillary qubits, which may be challenging given the limited number of qubits in current early-generation quantum computers.

Nevertheless, with advancements in Qiskit, researchers now have the ability to directly manipulate qubits using specific pulses and readout operations. This opens up opportunities for developing algorithms that tailor generalized circuits to specific circuit configurations based on input parameters and the properties of the quantum computer, such as its topology and gate errors.

4. Conclusions

In summary, there have been significant improvements in IBM quantum computers over the past two years. Previous experiments conducted two years ago resulted in correct outputs for two-qubit additions at a rate lower than 25%. However, in the current year, the upgraded quantum computers demonstrate higher correctness percentages. It is worth noting that the devices have the same qubit topology.

The Qiskit library has evolved to provide more comprehensive data about the physical device characteristics of each qubit. This information can be utilized for simulation purposes as well. The topology of qubits in a quantum computer plays a role in noise tolerance, with T-shaped topologies generally exhibiting better noise resilience than linear topologies.

The proposed generalized adder circuit incorporates a control rotation operation gate between every pair of qubits. It is observed that in the transpilation process, additional gates are added when two-qubit operations are not directly connected. These added gates can introduce noise into the system.

In quantum computing, building a quantum circuit requires an understanding of the physical architecture of the actual quantum computer, which distinguishes it from classical computing. The experimental results highlight the differences in behavior between simulators and

actual quantum computers, particularly when dealing with larger inputs. Knowledge of the physical properties of quantum computers enables researchers to gain insights into the current state of the noisy intermediate-scale quantum (NISQ) era and comprehend the effects of various types of noise, including environmental noise, noise from quantum mechanical processes, and noise from qubit control.

5. Acknowledgements

We would like to express our gratitude to the members of our lab, CU ISL, for their contributions in fostering the quantum community in Thailand. We also extend our appreciation to IBM Quantum for providing access to their services, which were instrumental in carrying out this research. It is important to note that the opinions and views expressed in this work are solely those of the authors and do not necessarily reflect the official policy or position of IBM or the IBM Quantum team.

References

[1] Grover, L.K., 1996. A fast quantum mechanical algorithm for database search. *Proceedings of the Twenty-Eighth Annual ACM Symposium on Theory of Computing.* Philadelphia, Pennsylvania, USA., May 22-24, 1996, pp. 212-219.

[2] Shor, P.W., 1997. Polynomial-time algorithms for prime factorization and discrete logarithms on a quantum computer. *SIAM Journal on Computing*, 26(5), https://doi.org/10.1137/S0097539795293172.

[3] Wikipedia, 2019. *RSA (cryptosystem).* [online] Available at: https://en.wikipedia.org/wiki/RSA_(cryptosystem).

[4] Draper, T.G., 2000. *Addition on a Quantum Computer*. [online] Available at: https://arxiv.org/abs/quant-ph/0008033.

[5] Vandersypen, L.M.K., Steffen, M., Breyta, G., Yannoni, C.S., Sherwood, S. and Chuang, I.L., 2001. Experimental realization of Shor's quantum factoring algorithm using nuclear magnetic resonance. *Nature*, 414(883-887), https://doi.org/10.1038/414883a.

[6] Beauregard, S., 2003. Circuit for Shor's algorithm using 2n+3 qubits. *Quantum Information and Computation*, 3(2), 175-185.

[7] Cross, A.W., Bishop, L.S., Smolin, J.A. and Gambetta, J.M., 2017. *Open Quantum Assembly Language.* [online] Available at: https://arxiv.org/abs/1707.03429.

[8] Cross, A.W., Bishop, L.S., Sheldon, S., Nation, P.D. and Gambetta, J.M., 2019. Validating quantum computers using randomized model circuits, *Physical Review A*, 100(3), https://doi.org/10.1103/PhysRevA.100.032328.

[9] Methachawalit, W. and Chongstitvatana P., 2020. Adder circuit on IBM universal quantum computers. *Proceedings of The 17th International Conference on Electrical Engineering/Electronics, Computer, Telecommunications and Information Technology,* Phuket, Thailand, June 24-27, 2020, pp. 92-95.

[10] Nielsen, M.A. and Chuang, I.L., 2011. *Quantum Computation and Quantum Information.* Cambridge: Cambridge University Press.

[11] Shor, P.W., 2003. Why haven't more quantum algorithms been found? *Journal of the ACM*, 50(1), 87-90, https://doi.org/10.1145/602382.602408.

[12] IBM Corporation, 2022. *IBM Quantum.* [online] Available at: https://quantum-computing.ibm.com.

[13] Qiskit, 2022. *Qiskit*. [online] Available at: https://qiskit.org.

[14] Qiskit, 2022. *qiskit.providers.aer.noise.NoiseModel.from_backend — Qiskit 0.37.1 documentation*. [online] Available at: https://qiskit.org/documentation/stubs/qiskit.providers.aer.noise.NoiseModel.from_backend.html#qiskit.providers.aer.noise.NoiseModel.from_backend.

[15] IBM Research, 2021. *The IBM Quantum Heavy Hex Lattice.* [online] Available at : https://research.ibm.com/blog/heavy-hex-lattice.

[16] Gambetta, J.M., Chow, J.M. and Steffen, M., 2017. Building logical qubits in a superconducting quantum computing system. *NPJ Quantum Information*, 3, https://doi.org/10.1038/s41534-016-0004-0.

[17] Bronn, N.T., Abdo, B., Inoue, K., Lekuch, S., Córcoles, A.D., Hertzberg, J.B., Takita, M., Bishop, L.S., Gambetta, J.M. and Chow, J.M., 2017. Fast, high-fidelity readout of multiple qubits. *Journal of Physics: Conference Series*, 834, https://dx.doi.org/10.1088/1742-6596/834/1/012003.

[18] Qiskit, 2022. *IBM Quantum*. [online] Available at: https://quantum-computing.ibm.com/services/resources?type=Falcon&system=ibmq_manila.

[19] Qiskit, 2022. *IBM Quantum*. [online] Available at: https://quantum-computing.ibm.com/services/resources?system=ibmq_quito.

[20] Qiskit, 2022. *Transpiler (qiskit.transpiler) — Qiskit 0.37.1 documentation*. [online] Available at: https://qiskit.org/documentation/apidoc/transpiler.html.